

# Integrated 2D photonic crystal stack filter fabricated using nanoreplica molding

Fuchyi Yang, Gary Yen, and Brian T. Cunningham\*

University of Illinois at Urbana-Champaign  
Department of Electrical and Computer Engineering  
Micro and Nanotechnology Laboratory, 208 N. Wright Street, Urbana, IL 61801, USA  
[\\*bcunning@illinois.edu](mailto:bcunning@illinois.edu)

**Abstract:** The design, fabrication, and characterization of an integrated 2D photonic crystal stack are described for application as optical filters with improved optical density and angle tolerance compared to single photonic crystal slabs. The 2D photonic crystals are designed as polarization independent reflectance filters with a narrow spectral bandwidth centered at  $\lambda = 532$  nm by utilizing the guided mode resonance effect. Up to three photonic crystal layers are vertically stacked upon a single plastic substrate by using repeated nanoreplica molding process steps, with no alignment required between stacked layers. The photonic crystal stack filters achieve optical density of 2.24 with an angular tolerance of 14.8 degrees.

© 2010 Optical Society of America

OCIS codes: (050.5298) Photonic crystals; (220.4241) Nanostructure fabrication

---

## References and Links

1. N. Ganesh, I. D. Block, and B. T. Cunningham, "Near ultraviolet-wavelength photonic-crystal biosensor with enhanced surface-to-bulk sensitivity ratio," *Appl. Phys. Lett.* **89**(2), 023901 (2006).
2. N. Ganesh, and B. T. Cunningham, "Photonic-crystal near-ultraviolet reflectance filters fabricated by nanoreplica molding," *Appl. Phys. Lett.* **88**(7), 071110 (2006).
3. I. D. Block, L. L. Chan, and B. T. Cunningham, "Photonic crystal optical biosensor incorporating structured low-index porous dielectric," *Sens. Actuators B Chem.* **120**(1), 187–193 (2006).
4. N. Ganesh, A. Xiang, N. B. Beltran, D. W. Dobbs, and B. T. Cunningham, "Compact wavelength detection system incorporating a guided-mode resonance filter," *Appl. Phys. Lett.* **90**(8), 081103 (2007).
5. P. C. Mathias, N. Ganesh, L. L. Chan, and B. T. Cunningham, "Combined enhanced fluorescence and label-free biomolecular detection with a photonic crystal surface," *Appl. Opt.* **46**(12), 2351–2360 (2007).
6. L. F. DeSandre, and J. M. Elson, "Extinction-Theorem Analysis of Diffraction Anomalies in Overcoated Gratings," *J. Opt. Soc. Am. A* **8**(5), 763–777 (1991).
7. A. Hessel, and A. A. Oliner, "A New Theory of Wood's Anomalies on Optical Gratings," *Appl. Opt.* **4**(10), 1275 (1965).
8. M. Neviere, P. Vincent, R. Petit, and M. Cadilhac, "Systematic Study of Resonances of Holographic Thin Film Couplers," *Opt. Commun.* **9**(1), 48–53 (1973).
9. M. C. Y. Huang, Y. Zhou, and C. J. Chang-Hasnain, "A surface-emitting laser incorporating a high-index-contrast subwavelength grating," *Nat. Photonics* **1**(5), 297 (2007).
10. M. C. Y. Huang, Y. Zhou, and C. J. Chang-Hasnain, "A nanoelectromechanical tunable laser," *Nat. Photonics* **2**(3), 180–184 (2008).
11. Y. Zhou, M. Moewe, J. Kern, M. C. Y. Huang, and C. J. Chang-Hasnain, "Surface-normal emission of a high-Q resonator using a subwavelength high-contrast grating," *Opt. Express* **16**(22), 17282–17287 (2008).
12. T. K. Lee, A. D. Bristow, J. Hubner, and H. M. van Driel, "Linear and nonlinear optical properties of Au-polymer metalodielectric Bragg stacks," *J. Opt. Soc. Am. B* **23**(10), 2142–2147 (2006).
13. N. N. Lepeshkin, A. Schweinsberg, G. Piredda, R. S. Bennink, and R. W. Boyd, "Enhanced nonlinear optical response of one-dimensional metal-dielectric photonic crystals," *Phys. Rev. Lett.* **93**(12), 123902 (2004).
14. I. D. Block, L. L. Chan, and B. T. Cunningham, "Large-area submicron replica molding of porous low-k dielectric films and application to photonic crystal biosensor fabrication," *Microelectron. Eng.* **84**(4), 603–608 (2007).
15. F. Yang, G. Yen, and B. T. Cunningham, "Voltage-tuned resonant reflectance optical filter for visible wavelengths fabricated by nanoreplica molding," *Appl. Phys. Lett.* **90**(26), 261109 (2007).
16. F. Yang, G. Yen, G. Rasigade, J. A. N. T. Soares, and B. T. Cunningham, "Optically tuned resonant optical reflectance filter," *Appl. Phys. Lett.* **92**(9), 091115 (2008).
17. B. Cunningham, P. Li, B. Lin, and J. Pepper, "Colorimetric resonant reflection as a direct biochemical assay technique," *Sens. Actuators B Chem.* **81**(2-3), 316–328 (2002).

18. B. Cunningham, B. Lin, J. Qiu, P. Li, J. Pepper, and B. Hugh, "A plastic colorimetric resonant optical biosensor for multiparallel detection of label-free biochemical interactions," *Sens. Actuators B Chem.* **85**(3), 219–226 (2002).
19. B. Cunningham, J. Qiu, P. Li, and B. Lin, "Enhancing the surface sensitivity of colorimetric resonant optical biosensors," *Sens. Actuators B Chem.* **87**(2), 365–370 (2002).
20. M. J. Grout, "Application of bacteriorhodopsin for optical limiting eye protection filters," *Opt. Mater.* **14**(2), 155–160 (2000).
21. M. Chen, C. F. Li, M. Xu, W. B. Wang, S. J. Ma, and Y. X. Xia, "Eye-protection glasses against YAG laser injury based on the band gap reflection of one-dimensional photonic crystal," *Opt. Laser Technol.* **39**(1), 214–218 (2007).
22. D. Rosenblatt, A. Sharon, and A. A. Friesem, "Resonant grating waveguide structures," *IEEE J. Quantum Electron.* **33**(11), 2038–2059 (1997).
23. S. Tibuleac, and R. Magnusson, "Narrow-linewidth bandpass filters with diffractive thin-film layers," *Opt. Lett.* **26**(9), 584–586 (2001).
24. V. N. Astratov, A. M. Adawi, S. Fricker, M. S. Skolnick, D. M. Whittaker, and P. N. Pusey, "Interplay of order and disorder in the optical properties of opal photonic crystals," *Phys. Rev. B* **66**(16), 165215 (2002).
25. J. W. Goodman, *Introduction to Fourier Optics*, 3 ed. (Roberts & Company, Englewood, 2005).
26. D. L. Brundrett, E. N. Glytsis, T. K. Gaylord, and J. M. Bendickson, "Effects of modulation strength in guided-mode resonant subwavelength gratings at normal incidence," *J. Opt. Soc. Am. A* **17**(7), 1221–1230 (2000).
27. F. Lemarchand, A. Sentenac, and H. Giovannini, "Increasing the angular tolerance of resonant grating filters with doubly periodic structures," *Opt. Lett.* **23**(15), 1149–1151 (1998).

## 1. Introduction

Reflectance filters based upon anomalous optical resonances that occur within certain periodic surface structures represent a class of devices that can, in theory, provide 100% reflection efficiency at a resonant wavelength. By selection of the grating period, the grating depth, the refractive index of the materials used in fabrication, and the thickness of dielectric thin films, resonance wavelengths can be engineered over a wide spectral range from UV [1,2] to IR [3–8]. Such devices, referred to as guided-mode resonance filters (GMRF), surface photonic crystals (PC), or PC slabs, are especially attractive as filters because they exhibit bandwidth and reflection efficiency that are similar to high contrast gratings [9–11] and multilayer Distributed Bragg Reflectance (DBR) filters [12,13], but can be fabricated using a 1D or 2D surface grating structure combined with a single high refractive index (RI) thin film deposition [14–16]. However, the period of the PC must be substantially less than the free-space wavelength of the filtered light, providing a challenge to inexpensive fabrication approaches, particularly for producing large device areas for visible wavelength applications. Recently, plastic-based nanoreplica molding has been applied to produce surface PC filters that enable production upon flexible sheets of plastic film in continuous rolls for application as optical biosensors [17–19].

Optical filters for protection of eyes or sensors are based on either absorption [20] or reflection [21] of incident laser radiation. For laser eye protection, the wavelengths of interest span from visible to near-IR, while protection of optical sensors used for thermal imaging and night vision are concerned with mid-IR wavelengths. Important parameters for these optical filters are optical density (OD), visible light transmission (VLT), and angular tolerance. OD is a quantitative measure of transmitted light based on a log scale,  $OD = -\log_{10}(T/T_0)$ , where  $T_0$  and  $T$  are the incident and transmitted light intensities, respectively. The American National Standards Institute (ANSI) regulates the required OD for different applications and environments in order to maintain laser irradiation below maximum permissible exposure (MPE) levels when entering the human eye. These standards are regulated under the ANSI Z136 series. For example,  $OD = 3$  is required to attenuate a continuous wave (CW) laser beam of  $2 \text{ mW/cm}^2$  to a transmitted intensity of  $2 \text{ } \mu\text{W/cm}^2$ , which is the maximum permissible exposure of the human retina to a green laser ( $\lambda = 532 \text{ nm}$ ).

Although computer models predict the possibility of 100% reflection efficiency for PC-based filters at their resonant wavelength [3,22], in practice, surface PC filters do not generally fully achieve this level of performance due to several factors. Materials used for PC fabrication may have small levels of optical absorption at the resonant wavelength that reduces resonance efficiency, the device period or duty cycle may be slightly imperfect over

the illuminated area, and nanometer-scale defects (such as particulate and voids) may contribute to non optimal behavior that is not well-modeled. Nonetheless, experimental demonstrations of surface PC filters routinely achieve reflection efficiencies in the range of 90-99% [1,15,16,23]. Therefore, one potential approach for obtaining OD greater than unity would be to integrate multiple surface PC filters onto a single substrate into a vertical stack, in which each layer of the stack reflects a substantial fraction of the light at a desired wavelength. Integrating multiple surface PC filters into a layered stack may also be used to broaden the angular full width half maximum (FWHM) of the system, in order to improve the angle tolerance of the device. This work presents the design, fabrication, and characterization of an integrated 2D PC stack filter with improved optical density and angular tolerance, designed to efficiently reflect a  $\lambda = 532$  nm laser. A 2-dimensional grating structure was selected so the reflectance response would be independent of incident light polarization for normal incidence. Also, compared to a DBR structure, this design can achieve similar OD while requiring substantially fewer thin film deposition steps, allowing a simpler and less expensive fabrication route for manufacturing optical limiting filters over large surface areas on flexible plastic materials. Precise fabrication of PC filter layers with identical resonant wavelength is enabled through the use of an *in situ* monitoring technique for measuring the resonant reflection peak during dielectric thin film deposition. This work represents, to the authors' knowledge, the first report of an experimentally demonstrated stacked PC filter used to obtain increased optical density (for a wavelength in the visible region of the spectrum). We show that stacking of PC filters can indeed be used to increase OD, but that each additional PC in the stack provides a diminished OD improvement due to lack of perfect collimation of the incident light source.

## 2. Fabrication

The device fabrication utilizes a nanoreplica molding process that requires the use of a silicon "master" wafer as a molding template [15,16,18]. The silicon master is a 6-inch diameter wafer upon which a 2D square lattice with 150 nm diameter circular posts and a period of  $\Lambda = 300$  nm was patterned by Deep-UV photolithography (North Carolina State University Nanofabrication Facility). The pattern is etched into the silicon wafer to a depth of  $d = 150$  nm by reactive ion etching to produce a 2D square lattice of posts. The silicon master is then used to replicate its nanostructures onto a target substrate. To do this, a layer of liquid acrylate UV-cured polymer (UVCP) was drop coated on top of the silicon master. A flexible polyethylene terephthalate (PET) substrate is then placed over the silicon master, and is next pressed into contact with the master using a rolling cylinder. This enables the UVCP drops to form a thin continuous layer between the two surfaces and conform to the features of the master. The UVCP is cured to a solid film by exposure to a high intensity UV lamp for 90 seconds. Next, the PET substrate is peeled away from the master, resulting in a cured UVCP layer with a square lattice of holes, period of  $\Lambda = 300$  nm, and duty cycle of 50% that is replicated onto the PET substrate. A SEM image of a UVCP nanoreplica mold is shown in Fig. 1(a) illustrating high integrity of the mold with few defects over many periods. An atomic force microscope (AFM) surface profile of the nanoreplica mold validates the PC period of  $\Lambda = 300$  nm in Fig. 1(b). The depth of the holes are close to 150 nm, but due to convolution with the AFM tip, it was not possible accurately determine the hole depth. The entire grating area produced by this method is  $5 \times 8$  cm<sup>2</sup> for the devices described here.

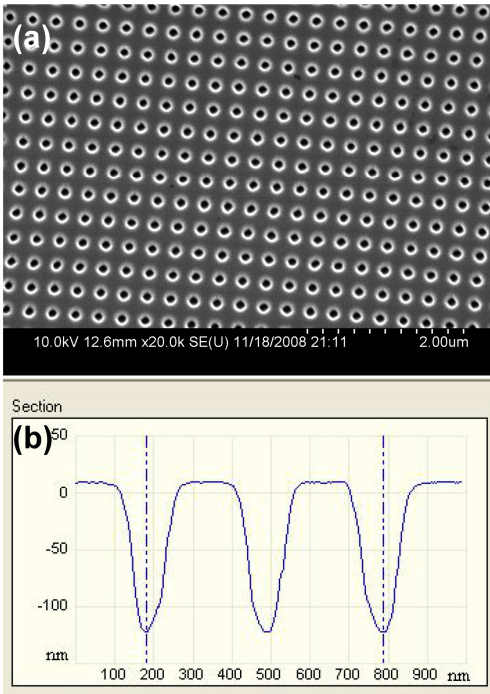


Fig. 1. (a) SEM view of the nanoreplica mold from a 2D square lattice photonic crystal silicon master. The master is comprised of posts resulting in a nanoreplica mold of 2D square lattice of holes. (b) AFM section view of nanoreplica mold showing a period of 300 nm and hole depth of approximately 150 nm.

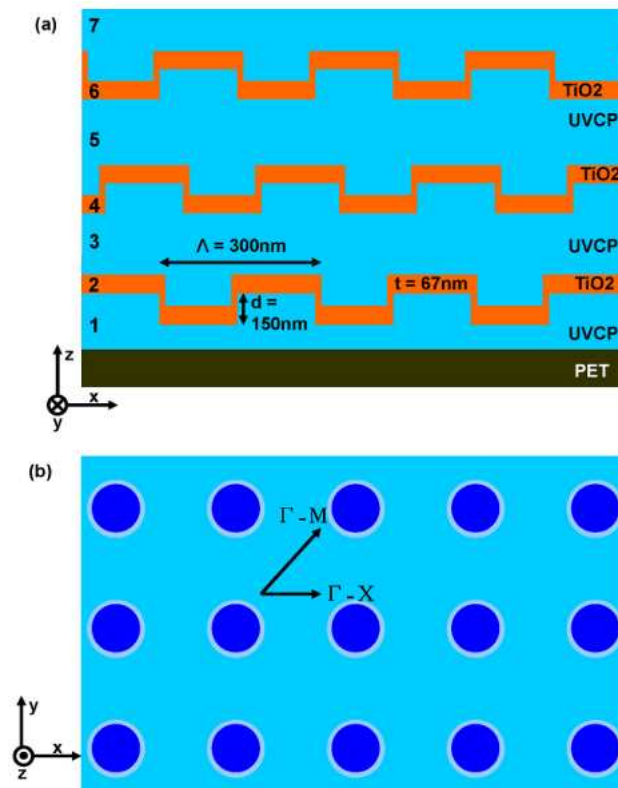


Fig. 2. (a) Cross section schematic view of a 3 PC stack filter with 300nm period, hole depth of 150 nm, and TiO<sub>2</sub> thickness of 67 nm. A single filter would consist of layers 1, 2, and 3 in the schematic. The schematic cross section is not to scale, as the UVCP layers (layers 1, 3, and 5) are each ~5 μm thick, and the PET substrate is ~250 μm thick. (b) Top view of the 2D PC filter with corresponding directions of the Brillouin zone with respect to the lattice vectors.

In order to produce a surface PC filter that produces resonant optical reflection, a high refractive index thin film must be deposited over the low refractive index ( $n = 1.45$ ) replica-molded grating structure. Here, sputter-deposited thin films of titanium dioxide (TiO<sub>2</sub>), with refractive index of  $n \sim 2.42$  at  $\lambda = 532$  nm, served as the high refractive index layer. In order to stack another layer on top of the first surface PC filter, a second nanoreplica molding step is performed on top of the TiO<sub>2</sub> layer, which produces an additional UVCP mold of 2D square lattice of holes. The replica molding/TiO<sub>2</sub> sequence may be repeated to generate a stack of surface PC filters with several layers, and stacks with  $N = 2$  PCs and  $N = 3$  PCs are demonstrated in this work. Figure 2(a) shows the cross section schematic for a filter consisting of 3 PCs and Fig. 2(b) is a top view of the same device structure. The thickness of the UVCP layers that are sandwiched between the TiO<sub>2</sub> films are ~5 μm, and are therefore substantially greater than the designed resonant wavelength. Because the individual PC layers are separated by a substantially large gap (compared to the resonant wavelength), there is no mode coupling between PC layers, and each layer behaves as an independent filter. Therefore, there is no requirement for tight tolerances for the thickness of the UVCP layer, and there is no requirement for lateral alignment of upper PC filters to the filters beneath them. In order to validate that integrated surface PC filters operate independently, we also measured the reflectivity performance of stacked surface PC that are individually fabricated upon separate substrates, and then characterized in series with ~8 cm gaps between each filter.

We refer to the resonant wavelength of a surface PC filter when illuminated with normal incident light as the center wavelength. The center wavelength depends on the parameters of the PC structure such as the period, hole depth, hole diameter, TiO<sub>2</sub> thickness, and the

refractive index of the UVCP and  $\text{TiO}_2$  layers. Since a silicon master is used for nanoreplica molding, most of these parameters are fixed, and the main variable in fabrication of the PC filters is the  $\text{TiO}_2$  thickness.

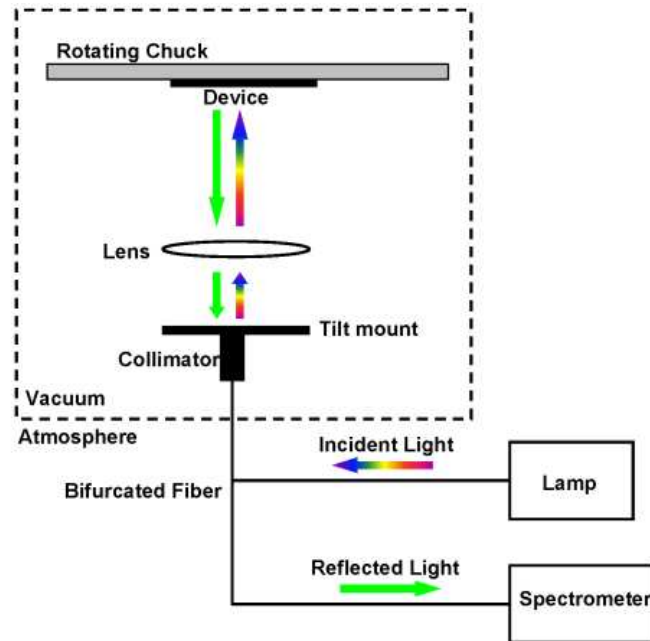


Fig. 3. Schematic of the *in situ* reflection spectrum monitoring system. The low vacuum environment is inside the dashed box. In one leg of the bifurcated optical fiber, incident light is illuminated onto the device through a collimator and lens optical system. The reflected light is collected through the same optics and sent to the other leg of the optical fiber, where it is measured with a spectrometer.

In order to produce PCs in the stack that have identical center wavelengths ( $\lambda = 532$  nm), strict control of the  $\text{TiO}_2$  thin film thickness is required for each deposition. For this purpose, an *in situ* monitoring system was developed to monitor, in real time, the reflection spectrum of the PC filter while depositing  $\text{TiO}_2$  in a sputtering chamber (see Fig. 3). Thus, the center wavelength was observed during the sputtering process and the process was stopped when it reached a desired value in a vacuum environment ( $\lambda = 505.39$  nm). This “vacuum” center wavelength would result in  $\lambda = 532$  nm, after the  $\text{TiO}_2$  film is overcoated with a UVCP layer. The monitoring system consists of a custom made bifurcated multi-mode optical fiber that includes an in-line vacuum feedthrough conflat flange in the sputter deposition chamber. The vacuum feedthrough allowed interfacing between inside and outside of the vacuum chamber. Inside the chamber, broadband light was illuminated through one optical fiber coupled to a collimator. An additional lens was placed in order to refocus the light before it was incident onto the PC filter. The PC filter is mounted on a chuck that rotates during sputtering. The reflected light was collected through the same collimator and into the other optical fiber. Outside of the vacuum chamber, a tungsten halogen lamp was connected to one leg of the bifurcated cable to supply incident light, while the other leg was connected to a spectrometer (Ocean Optics) to acquire the reflection spectrum of the device during  $\text{TiO}_2$  sputter deposition. Using this monitoring setup, it was possible to control the center wavelength among different PC filters in the stack to within  $\Delta\lambda = 1$  nm.

### 3. Experiment

The devices were characterized using a transmission setup, as depicted in Fig. 4, using broadband incident light from a tungsten halogen lamp coupled to a fiber optic cable. The

incident light was unpolarized and collected on the transmitted side using another fiber optic cable which was connected to a spectrometer. The spectrometer output was observed using commercial software from Ocean Optics. The PC filters were mounted on a rotating stage which allowed adjustment of the angle of incident light in the  $xz$  plane as referenced in Fig. 2(a). Even though there are additional methods of characterizing the transmission of the filter as a function of incident angle [24], this method was sufficient for the intended purpose. Also, the PC filter was attached to a tilt mount which enabled adjusting the filter to normal incidence with respect to the incoming light.

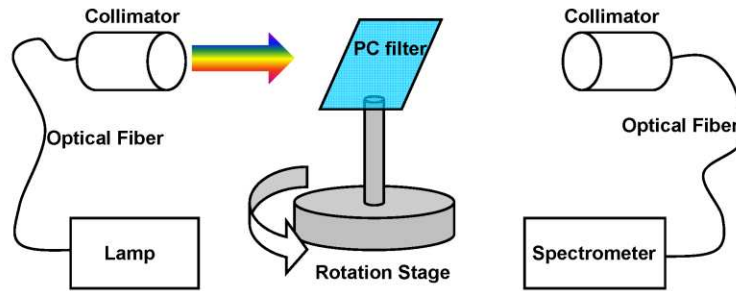


Fig. 4. Setup used to acquire the transmission spectrum of the PC stack filter during different stages of the fabrication process. Broadband light from a tungsten halogen lamp is incident on the device and the transmitted light is collected and analyzed using a spectrometer.

The first device tested was a 3 PC stack filter with each PC filter in the stack having a center wavelength of  $\lambda = 532$  nm. This was achieved by depositing approximately 67 nm of  $\text{TiO}_2$  for all 3 PCs. The goal of this design is to increase the OD of the PC filter at the target wavelength as the number of PC layers increases. Ideally, the OD of the overall filter should scale linearly with the number of PC filters as shown in Eq. (1):

$$OD_n = -\log_{10} \left( \frac{T^n}{T_o} \right) = -n \cdot \log_{10} \left( \frac{T}{T_o} \right) = n \cdot OD_1 \quad (1)$$

where  $T^n$  is the transmission efficiency for a stacked device of  $n$  PC layers, and  $T_o$  is 100% transmission efficiency. The transmission spectrum at normal incidence was recorded during the fabrication process, after completion of each PC filter in the stack. The fabrication of subsequent PC filters resulted in increased OD at the target wavelength as seen on the transmission spectra in Fig. 5(a), increasing from  $OD = 1.45$  with a single PC filter to  $OD = 2.24$  with a 3 PC stack filter. This improvement shows that stacking PC filters is a feasible solution to improving the OD of PC filters.

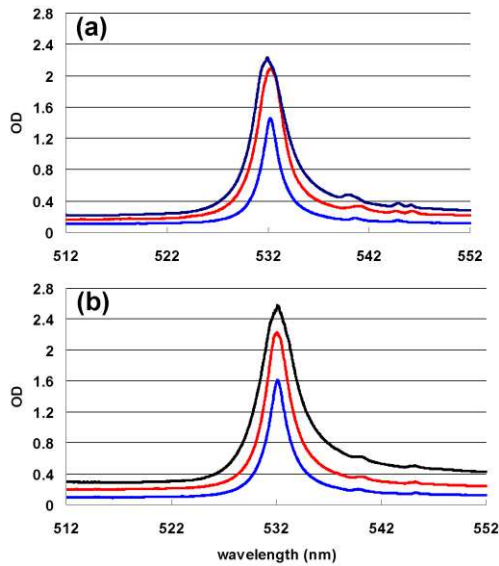


Fig. 5. (a) OD spectrum of a PC stack filter during the fabrication process with the filter comprising  $N = 1$  (blue line),  $N = 2$  (red line), and  $N = 3$  (black line) PC filters. OD increases from 1.45 to 2.24 by stacking 3 PC filters. (b) OD spectrum of 3 discrete PC filters with 1 (blue line), 2 (red line), and 3 (black line) PC filters in the optical transmission pathway. The OD increases from 1.61 to 2.58.

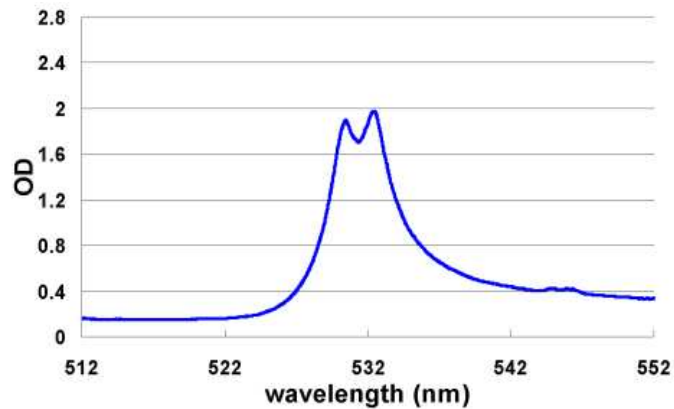


Fig. 6. OD Spectrum of a 2 PC stack filter. The center wavelengths of the two different layers are intentionally offset by 2 nm in order to increase the angular tolerance of the reflectance filter.

The second device tested was a 2 PC stack filter where the reflection peaks are offset at half width half maximum (HWHM) apart; Fig. 6 shows the OD spectrum which depicts one peak at  $\lambda = 530$  nm and another at  $\lambda = 532$  nm. The wavelengths of the reflection peaks were controlled by depositing the appropriate amount of  $\text{TiO}_2$  for each PC. This device was designed to increase the angular tolerance of the PC filter by designing the OD spectrum to exhibit a broad and flat OD peak. A reference device with a single PC and reflection peak at the same wavelength was also fabricated for comparing angle tolerance. The transmission spectrum of the devices was recorded using the setup described above. A series of spectra was taken at different incident angles ranging from  $-10^\circ$  to  $+10^\circ$  at a resolution of  $0.1^\circ$ . Changing the incident angle of light changes the propagation constant and wavelength of the resonantly excited PC mode which produces the optical limiting effect. The optical resonances occur along the bands of the PC and are therefore a function of angle and wavelength. We were able



to plot the band diagram of the PC filter along both  $\Gamma$ -X and  $\Gamma$ -M directions of the 2D square lattice PC which is shown in Fig. 7. These dispersion plots contain complete spectral and angular transmission spectrum of the devices. Taking a vertical slice through the band diagram results in a transmission spectrum over a range of wavelengths and at a single incident angle. By taking a horizontal slice through the band diagram, we observe the transmission spectrum over a range of angles at a single wavelength. At the center wavelength, the PC filter has an OD peak as a function of angle. The FWHM of this peak is a measure of the angular tolerance of the device. With this in mind, the angular transmission spectrum at the center wavelength was obtained for the 2 PC stack filter and a reference PC filter and plotted in Fig. 8. The angle tolerance of the 2 PC stack filter improved due to the increased angular FWHM from  $\Delta\theta = 6.8^\circ$  to  $\Delta\theta = 9.1^\circ$  in the  $\Gamma$ -M direction and from  $\Delta\theta = 9.4^\circ$  to  $\Delta\theta = 14.8^\circ$  in the  $\Gamma$ -X direction. The  $\Gamma$ -X FWHM is larger than the  $\Gamma$ -M FWHM due to the presence of a flat band which retains its guided mode resonance in the orthogonal plane to the incident plane.

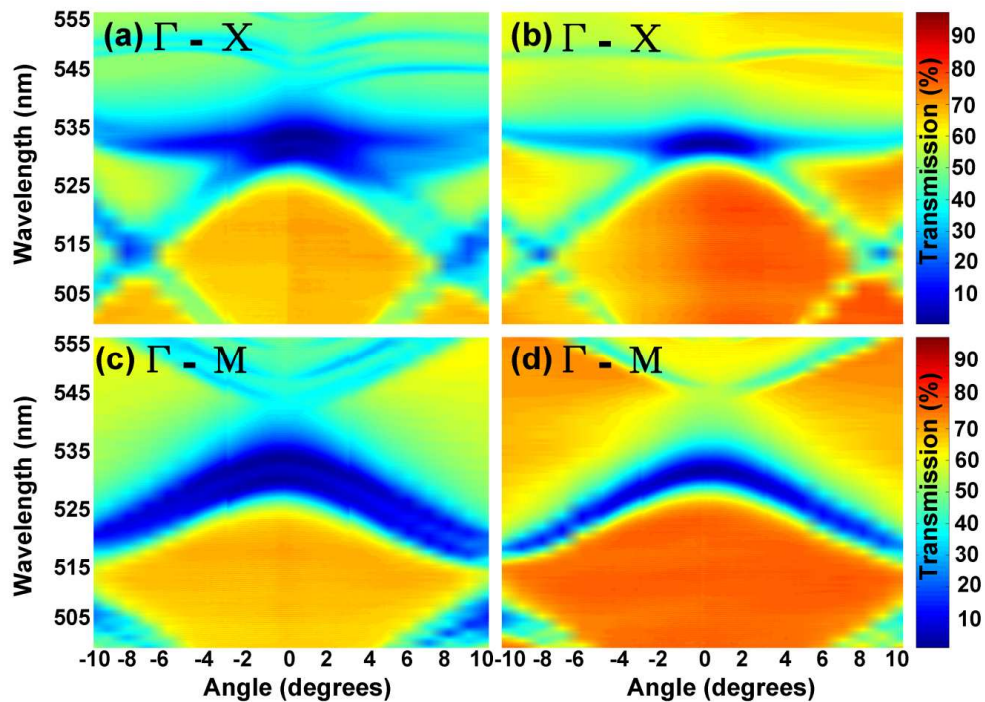


Fig. 7. Band diagram of the 2D PC filter in the  $\Gamma$ -X (plots a & b) and  $\Gamma$ -M (plots c & d) directions. Color scale represents 0% transmission (blue) to 100% transmission (red). The  $\Gamma$ -X band diagram has a flat band effect that is clearly not seen in the  $\Gamma$ -M direction. The reference device (plots b & d) has smaller angular FWHM than the stack PC filter (plots a & c) due to its smaller resonance line width that is seen in the band diagram.

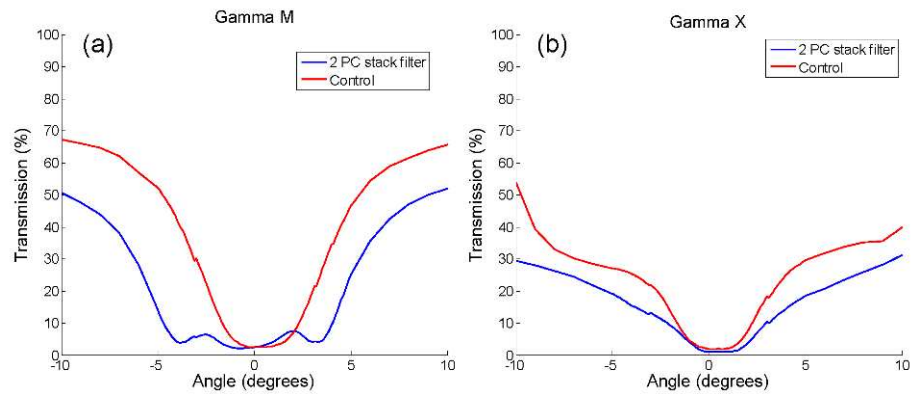


Fig. 8. Angular transmission response of a 2 PC stack filter (blue) and control PC filter (red) at the center wavelength. (a)  $\Gamma$ -M direction response showing improved angular tolerance for the 2 PC stack filter. (b)  $\Gamma$ -X direction response showing improved angular tolerance for the 2 PC stack filter.

#### 4. Discussion

The PC stack filter was shown to increase its OD with each additional PC filter in the stack. However, it is evident that the increase in OD is not as dramatic as suggested by Eq. (1). One potential cause for the discrepancy between an ideal structure and the experimentally measured structure is that the center wavelengths among the PC filters do not match precisely, since they vary within  $\Delta\lambda \sim 1$  nm due to slight differences between the sputtered  $\text{TiO}_2$  thicknesses. The optical resonance has a spectral FWHM  $\Delta\lambda \sim 5$  nm, so a mismatch of  $\Delta\lambda \sim 1$  nm between center wavelengths will decrease the transmission efficiency appreciably. With perfect overlap, a filter comprised of 3 PC filters in series would achieve OD values closer to the values predicted by Eq. (1).

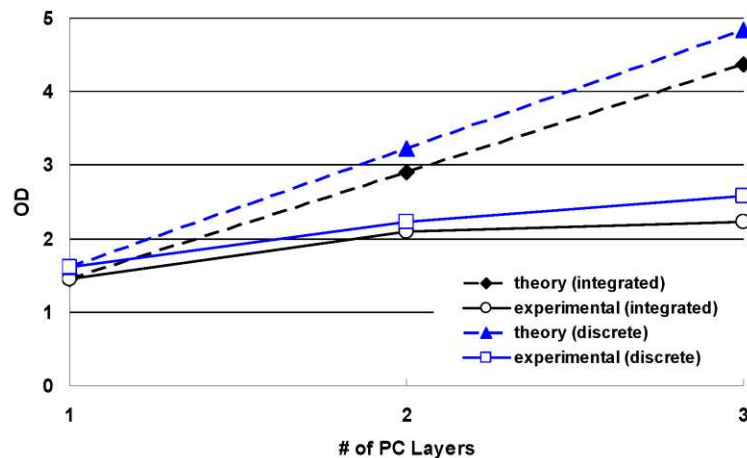


Fig. 9. Comparison between theory and experimental data for increase in OD as a function of number of PC filters in a stack. The experimental results are lower than the predicted values and show a diminishing increase in OD with additional PC filters incorporated into the stack.

In order to investigate this issue further, three individual PC filters were fabricated on separate PET substrates. These filters have matching center wavelengths at  $\lambda = 532$  nm. These 3 discrete PC filters were mounted individually on tilt mounts and placed in the transmission setup described earlier. The spacing between the PC filters was 8 cm. The OD spectra of the filters were recorded with 1, 2, and 3 PC filters placed in the transmission path as shown in

Fig. 5(b). The OD improves from  $OD = 1.68$  with single PC filter to  $OD = 2.58$  with 3 discrete PC filters. Figure 9 compares the theoretical and experimental OD increases as a function of number of PC filters in the stack. Using these separate PC filters, the result was similar to an integrated PC stack filter. Both cases show OD values less than predicted along with diminished increase in OD with each additional PC filter. Since both cases exhibit the same behavior, we can eliminate the possibility that optical coupling between PC filters is responsible for the observed reduced OD because the PC filters are separated by 8 cm. Also, Fabry-Perot effects can be eliminated from consideration since the spacing between PC filters was not designed as multiples of quarter or half wavelengths of the resonant light.

Using three discrete PC filters, we observed that the wavelength of light that was resonant with the first PC filter in the transmission setup was less efficiently blocked by the second and third PC filters. Figure 10 shows the OD spectra of each PC filter in the series referenced to its incident light. The first PC blocked 97.5% of the incident light from the optical fiber, the second PC blocked 76% of its incident light (light passing through the first PC), and the third PC blocked 55% of its incident light (light passing through both the first and second PC). Therefore, when the three PC layers are designed to have the same center wavelength, each additional PC layer results in diminishing increases in OD. However, non-resonant light gave the same transmission efficiency for all three PC filters. The effect of diminishing increases in the OD can be explained as follows. In the computer model, the incident light is comprised of a perfect plane wave incident upon the PC at normal incidence, with no components at oblique incidence. The OD peak of a single PC filter has a limited angular FWHM when the response of the PC is plotted for transmission as a function of incident angle at the center wavelength. This is due to the optical resonance being a function of both wavelength and angle as mentioned previously. Additionally, the incident light is not a pure plane wave, but has a Gaussian mode profile that can be represented by its angular wave spectrum [25]. The angular wave spectrum is the spatial Fourier representation of the wave front with the Fourier basis being plane waves in different propagation directions. Thus, a Gaussian mode profile can be deconstructed into its angular wave spectrum consisting of plane waves at different incident angles and amplitudes. At the center wavelength, the PC filter is able to efficiently block incident plane wave components that are nearest to normal incidence. This fact results in plane wave components which are oblique to be transmitted through the first PC filter and become incident on the second PC filter. These plane waves which are at the center wavelength but at oblique incidence to the second filter have higher transmission efficiency due to the limited angular tolerance of the PC filter. The result is that the second PC filter blocks less of its incident light than the first PC filter. The same argument holds when interpolating to the additional PC filters with each additional PC filter blocking increasing less of its incident light than the PC filter before it. This is the most important reason why the experimental data deviates from theory, and places a limit on the number of PC filters that can be stacked effectively in practice.

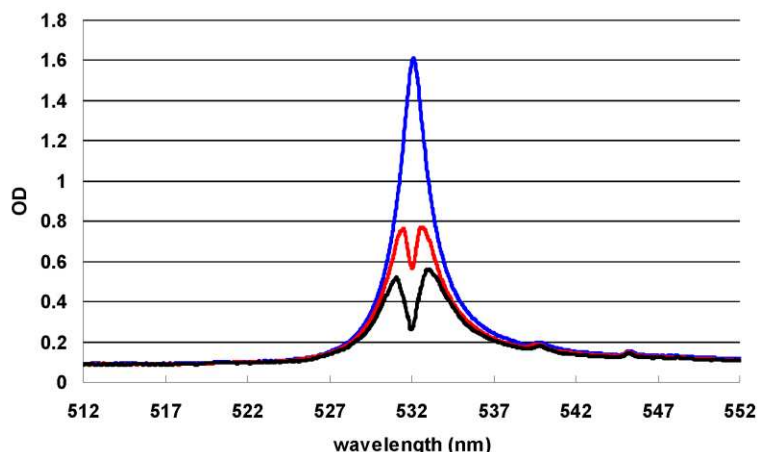


Fig. 10. OD spectrum of a 2D PC filter when the incident has been transmitted through 0 (blue line), 1 (red line), and 2 (black line) PC filters before reaching the current PC filter.

Because the OD improvement is limited by the finite angular FWHM of the PC, one way to overcome this limitation is to increase the PC filter's angular FWHM. This can be done by increasing the spectral FWHM of the stack PC filter by designing the different PC layers to have staggered center wavelength resulting in an effective resonance that is wider. This can be done by varying the  $\text{TiO}_2$  thickness of each PC layer in order to obtain the desired center wavelengths. As Fig. 7 shows, a wider FWHM in wavelength corresponds to a broader FWHM in angle, increasing its angular tolerance. Also, it is possible to design the PC filter to have a flatter dispersion at the band edge which will increase the angular FWHM. The band edge corresponds to the center wavelength value. A flatter dispersion means that the optical resonance's wavelength doesn't vary as much as a function of angle, increasing the PC filter's angular tolerance at the center wavelength. This has been studied previously and it has been shown that optimizing the duty cycle of the PC to certain values can flatten the dispersion to improve angular tolerances of PC filter in theory [26,27].

The PC filter has a spectral FWHM  $\Delta\lambda \sim 5$  nm. This is an advantage over DBR stacks which typically have larger bandwidths for their stop bands. The PC filter can effectively block a narrow band of wavelengths around the center wavelength while transmitting a wider range of wavelengths in the visible spectrum. Thus, it is possible to maintain a sufficient level of visibility and color integrity while simultaneously optical limiting 532 nm wavelength light.

Another consideration is the effect of light which is not resonant with the 2D PC structure. Stacking PC filters results in large discontinuities of refractive index in the  $z$  direction as defined in Fig. 2(a), where each PC region effectively behaves as a thin film interference structure with a reflectivity that is wavelength dependent. As the number of PC filters increases, the number of layers of discontinuous refractive indices also increases, resulting in a highly complex reflection spectrum over a broad wavelength band. Because the UVCP layer thicknesses are not precisely controlled, the multi-PC stack does not behave as a distributed Bragg reflector, although computer simulations show that bands of high and low reflection efficiency will form at wavelengths other than the resonant wavelength. These bands are undesirable since they reduce the transmission of light which do not couple into the 2D PC layers and should pass through the PC stack filter, and are particularly undesirable if the bands fall within the visible spectrum, as they will reduce transmission efficiency for wavelengths other than the resonant wavelength, thus decreasing overall visibility through the filter.

When the PC layers are stacked by repeated nanoreplication steps, alignment between the principal axes of the 2D lattice was not strictly controlled among the multiple PC filters. For example, in Fig. 2(b) the  $\Gamma$ -X direction of each PC layer was not aligned to one another. This has no effect for the transmission spectrum at normal incidence. The OD peak remains at the

center wavelength at normal incidence regardless of the incoming light polarization since the 2D PC is symmetric in both  $x$  and  $y$  directions. However, at oblique incidence, the OD peak varies in wavelength when the angle is varied. This effect limits the angular tolerance of the PC filter. The following proposed design can result in improved performance. For a single PC filter, the dispersion in the  $\Gamma$ -X direction contains flat bands at the center wavelength as seen in Fig. 7(a) and 7(b) at the center wavelength of  $\lambda = 532$  nm. This behavior is not seen in the dispersion along the  $\Gamma$ -M direction. The flat band is beneficial because it allows the PC filter to maintain effective optical limiting at the center wavelength even at oblique incidence angles. When fabricating PC filters, offsetting each PC layer's principal axes relative to the others can maximize the effect of the flat band in as many directions as possible. In the case of two PC layers, the second PC layer should rotate its principle axis by  $45^\circ$  relative to the first PC layer, resulting in the  $\Gamma$ -X axis of the second PC layer lining up with the  $\Gamma$ -M axis of the first PC layer. Overlapping the Brillouin zones of the PC layers in this manner would maximize the number of directions in the  $xy$  plane which exhibit the flat band. Thus, the angular tolerance of the filter can be improved even further.

## 5. Conclusion

Integrated 2D PC filter stacks were fabricated using nanoreplica molding which enabled fabrication onto large area and flexible substrates. Improved OD at a target wavelength of  $\lambda = 532$  nm was demonstrated by designing a filter with three PCs in series with each PC having reflection peak at the same wavelength. Increased angle tolerance was achieved by designing a 2 PC stack filter with each PC having reflection peak wavelengths offset by approximately the HWHM. Both of these concepts can be combined onto a single substrate to create a high OD filter with improved angle tolerance. Further improvements to this approach were discussed including increasing the angular tolerance through optimization of the duty cycle of the PC and alignment between PC layers to take advantage of the flat bands in the 2D PC dispersion. In principle, each PC in a vertical stack serves to increase the OD, but with diminishing improvement for each PC due to the low angular tolerance of a single PC combined with incident light that is not strictly comprised of collimated plane waves. By staggering the center wavelength through manipulation of the  $\text{TiO}_2$  dielectric film thickness, greater angular tolerance is achieved, suggesting the possibility of using a substantially greater number of stacked PCs to obtain further increases in OD.

## Acknowledgments

The research was supported by the U.S. Army under project manager Dr. Joel Carlson under contract W911QY-06-C-0043, and acknowledge Dr. Carlson for many helpful discussions. Also, fabrication support was received from the North Carolina State Nanofabrication Facility.